*Journal of Structural Geology*, Vol. 5, No. 3/4, pp. 419 to 430, 1983
Printed in Great Britain

0191-8141/83 \$3.00 + 0.00
Pergamon Press Ltd.

# Strain patterns of crescentic granitoid plutons in the Archean greenstone terrain of Ontario

W. M. SCHWERDTNER

Department of Geology, University of Toronto, Toronto, Ontario, Canada M5S 1A1

G. M. STOTT

Ontario Geological Survey, 77 Grenville Street, Toronto, Ontario, Canada M5S 1B3

and

R. H. SUTCLIFFE

Department of Geology, University of Western Ontario, London, Ontario, Canada N6A 5B7

(*Received* 15 *June* 1982; *accepted in revised form* 14 *January* 1983)

**Abstract**—Granitoid plutons of crescentic outcrop pattern in the Archean terrain of northwestern Ontario are dominated by constrictive strains that are interpreted to be due to intrusion rather than regional deformation. The strain patterns of antiformal plutons are characterized by subvertical lineations. In contrast, the strain patterns of synformal plutons are characterized by subhorizontal lineations. Presumably, only the last flow increments were recorded by the deformed mineral aggregates employed as strain gauges, and occurred when the granitoid magma was largely crystalline. Simple kinematic models are capable of explaining many but not all elements of the natural strain patterns.

## INTRODUCTION

THE ARCHEAN peneplain terrain of northwestern Ontario, Canada, is characterized by numerous greenstone belts and intervening gneiss domains which include granitoid plutons ranging in composition from granite to diorite (Blackburn 1981). The plutonic rocks contain xenoliths of gneiss and greenstone. Before the intrusion of most, if not all plutons (Schwerdtner *et al.* 1979), the gneiss domains were aggregates of domes and related structures (Schwerdtner & Lumbers 1980, Schwerdtner 1982). Many gneiss domes are now partly surrounded by granitoid bodies of crescentic horizontal outline, which have been called "crescentic granitoid plutons" (Schwerdtner *et al.* 1979).

The complete three-dimensional geometry of the crescentic granitoid plutons is unknown. Judging from the dip of foliation and other planar structures near their intrusive contacts (Schwerdtner *et al.* 1979, fig. 9), the exposed portions of most plutons are conical to quasi-cylindrical sheets. They seem to have the form of single members in steeply plunging rootless folds that are upright to slightly inclined. In analogy with such folds, we distinguish between antiformal and synformal (crescentic) plutons. Antiformal plutons flank upright gneiss domes that have no overhang; synformal plutons are moulded to the overhanging side of inclined gneiss domes or incipient gneissic nappes. Other plutons seem to be funnel-shaped for they have a synformal boundary with their metavolcanic envelope but an antiformal boundary with the gneiss domes.

In map view, some crescentric plutons have (1) constricted 'hinge zones' or (2) thick, axial-planar arms of metavolcanics. These features suggest that two parasitic structures have emerged from a large crescentic pluton injected between a stable gneiss dome and its greenstone envelope. If this hypothesis proves to be correct then situation (1) would represent a level of exposure that is close to the root zone of the parasitic structures (plutonic lobes).

The hypothesis of *plutonic injection after the gneiss doming* is supported by field observations which suggest that most crescentic plutons postdate the last penetrative deformation of the surrounding greenstone belts. For example, some granitoid apophyses of the crescentic plutons contain *equant* angular xenoliths of the metavolcanic wall rocks that appear to postdate the last penetrative deformation of the greenstone belts. Where the regional structural history has been established (Stott & Schwerdtner 1980), the largest metavolcanic xenoliths seem to contain a record of the entire penetrative deformation of a given greenstone belt.

Many crescentic plutons have metamorphic aureoles. Planar granitoid apophyses are neither folded nor boudined. The mineral aggregates of apophyses are commonly undeformed. Where slightly to moderately strained, the mineral-elongation directions in granitoid apophyses are markedly oblique or subperpendicular to the regional extension directions in the adjacent greenstone. Structural elements of regional deformation in greenstone belts, including discrete late-stage shear zones and kink bands, are invariably absent from crescentic plutons (Stott & Schwerdtner 1980). We shall attempt to show that the strain pattern of the plutons is in fact compatible with originally crescentic forms.

*Strained and unstrained granitoid rocks*

The mineral constituents of the granitoid rocks are virtually undeformed throughout some of the crescentic plutons studied. Clearly, the strongly crescentic shape of such plutons could not have been attained by folding of consolidated arcuate or tabular sheets. Three other alternatives cannot be ruled out: (i) in-situ folding of molten tabular bodies together with their wall rocks; (ii) magma generation at, and magma ascent along, the gneiss–greenstone interface of domes and (iii) injection of magma into, and further rise along, the arcuate gneiss–greenstone interface. All these alternatives require that the granitoid magma was at rest in the final stages of crystallization and consolidation of the plutons. In addition, the unstrained crescentric plutons must postdate the latest penetrative deformation of the gneiss domes and greenstone belts (cf. Schwerdtner *et al.* 1979, pp. 1972–1973).

Most crescentic plutons exhibit deformed mineral aggregates and other evidence of pervasive strain in a solid or nearly-solid state. Is this strain indicative of diapiric bending of early granitoid sills, a marked change in average radius of crescentic plutons, or the flow of nearly solid magma in the final stages of plutonic intrusion? Answers to this question have been sought, in the present study, by investigating the strain patterns of the plutons.

Our research has been greatly hampered by the lack of published strain models applicable to large folds. Most published models were made without regard to the effects of gravity, and are therefore inapplicable to large or even batholith-size plutons. Many analogue models of gneiss diapirs, in turn, neglect the effect of horizontal tectonic compression in the earth's crust. In spite of this deficiency, these models may be applicable to Archean gneiss domes. If so, one should be able to test whether crescentic plutons with strained mineral aggregates are folded sills that had been emplaced, prior to diapirism, between a gneiss complex and its greenstone cover.

Simple kinematic models were constructed to test the possibility that the crescentic plutons rose along the arcuate interface of gneiss domes. These models consider the geometry of flow regimes, but ignore the rheologic state and boundary conditions of the magma. They are, therefore, incapable of predicting the strain near plutonic margins.

In three accessible plutons, we mapped the trajectories of principal strain and estimated the range of the prolateness factor $k$ (Flinn 1962) of the strain ellipsoid by inspection of large rock specimens. Strain analyses made in the laboratory gave an indication of the average strain within the plutons as well as permitting a check of the range of $k$ as judged in the field.

The first of the three intrusions studied is situated in western Wawa Subprovince, the others are located in the Wabigoon Subprovince, NW Ontario. The first intrusion has the form of an upright conical antiform, the second an upright synform and the third a large synform with a constricted hinge zone. To complement our treatment of this constricted structure, we also give a brief description of a comparable antiformal pluton.

## GREENWATER LAKE PLUTON: EXAMPLE OF AN ANTIFORMAL STRUCTURE

The Greenwater Lake Pluton (GLP) resembles a steeply plunging conical antiform (Figs. 1 and 2). It constitutes a good example of a single intrusion with several compositional variants, and is situated in the south-central portion of the Shebandowan greenstone belt, Ontario (Stott & Schwerdtner 1980, Schwerdtner *et al.* 1978a). Much of this crescentic pluton is covered by the arcuate Greenwater Lake (Schwerdtner *et al.* 1978a, fig. 5), but there are sufficient islands and reefs to ascertain the overall shape and lithology of this intrusive body. The eastern segment of the convex contact underlies the lake.

The interior of the GLP is a hornblende–biotite granodiorite with polycrystalline quartz eyes, whereas the marginal domains are composed of diorite or quartz-monzodiorite containing hornblende and/or biotite as well as feldspar megacrysts. Commonly, the mafic minerals are concentrated in clots or xenoliths of amphibolite and metahornblendite. Most xenoliths have average diameters of 5–15 cm, and conform in shape and orientation to the mineral shape fabric. This fabric conformity suggests a coaxial strain path unless (1) the xenoliths have been corroded mechanically or chemically in the late stages of intrusion or (2) the strain is related to in-situ deformation of the GLP.

Quartz eyes in the granodiorite rocks are polycrystalline aggregates (3–8 mm in diameter) whose strain

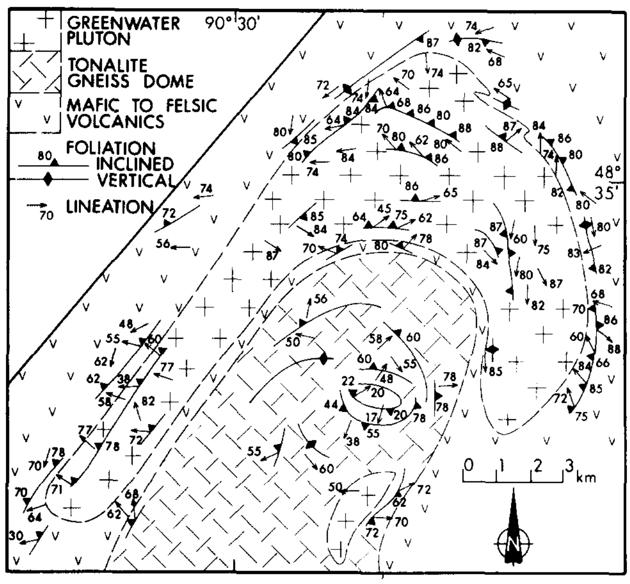


Fig. 1. Lithology and structure of the Greenwater Lake Pluton, Shebandowan greenstone belt, Ontario, Canada.

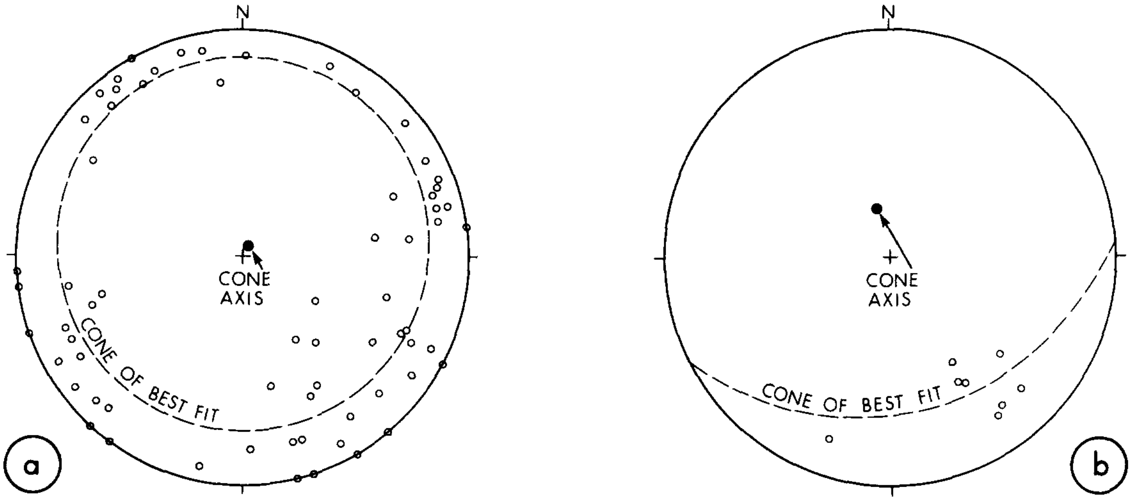


Fig. 2. Shape of the Greenwater Lake Pluton (Fig. 1). Best-fit small circles (after Ramsay 1967, p. 20) with apical angles of 80 and 94° in equatorial equal-angle projection: (a) foliation poles near convex boundary; (b) foliation poles near concave boundary.

has been estimated using Robin's (1977) method. Sample locations are shown in Fig. 3, and results are summarized in Table 1. Strain intensities will be referred to as $r$-values (Watterson 1968) and range from 1.10 to 3.35 (Fig. 4).

The pattern of $k$ values (Flinn 1962) is symmetric within the GLP (Fig. 4). The central zone of the GLP is one of constrictive strain whereas the contact regions possess minimal $k$ values, reflecting predominantly flattening strain. Although $r$-values reach a maximum in the contact regions, the central domain has also been strained and did not experience simple plug flow. Directions of maximum extension are subparallel to the dip trajectories of the antiform (Fig. 1).

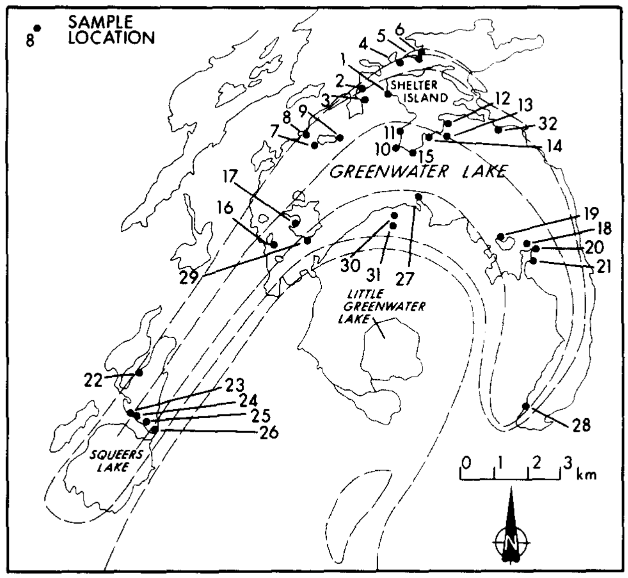


Fig. 3. Sample locations of Table 1 for the Greenwater Lake Pluton.

## McNEVIN PLUTON: EXAMPLE OF A SYNFORMAL STRUCTURE

The McNevin Pluton (MP) is sandwiched between a pair of arcuate greenstone arms (Fig. 5) that emerge from the Lumby Lake metavolcanic-metasedimentary belt (Woolverton 1960). Gneissic and weakly strained granitoid rocks occur on the concave side and gneissic tonalite–granodiorite on the convex side of this sandwich structure (Fig. 5). The MP is composed of buff granodiorite with polycrystalline quartz eyes (Fig. 6).

While the easternmost part of the MP is covered by the Lac Seul moraine north of the Trans-Canada Highway, the southern end is exposed on the eastern shore of Upper Scotch Lake (Fig. 5). The poles to the transposed primary layering and foliation in the greenstone envelope, on both sides of the MP, define a partial girdle whose cone axis is subvertical (Fig. 7). The 'hinge' of the pluton (Fig. 5) plunges about 75° SE. Therefore, the MP is a simple synformal sheet that plunges away from the gneiss terrain and toward the Lumby Lake belt.

Apart from pink aplitic veins and unstrained felsic and intermediate dykes, the MP is a single-phase granodioritic intrusion which is finer grained near the contacts.

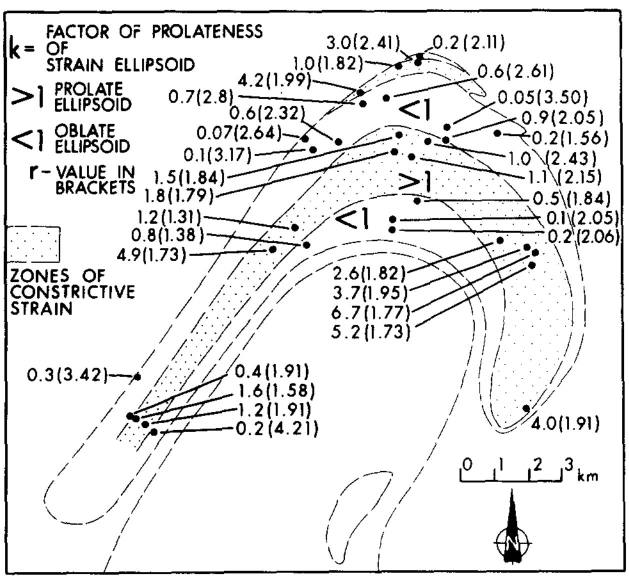


Fig. 4. Fields of $k$ and $r$ in the Greenwater Lake Pluton.

Table 1. Strain analysis, Greenwater Lake Pluton

| Sample No. | $X/Z$ | $X/Y$ | $Y/Z$ | $r$ | $k$ | $\gamma_0$ | $\nu$ |
|---|---|---|---|---|---|---|---|
| GMS 1 | 3.23 | 1.62 | 1.99 | 2.61 | 0.60 | 0.96 | 0.17 |
| GMS 2 | 2.14 | 1.80 | 1.19 | 1.99 | 4.20 | 0.65 | −0.54 |
| GMS 3 | 3.60 | 1.77 | 2.03 | 2.80 | 0.70 | 1.05 | 0.11 |
| GMS 4 | 2.00 | 1.40 | 1.42 | 1.82 | 1.00 | 0.56 | 0.02 |
| GMS 5 | 2.97 | 2.06 | 1.35 | 2.41 | 3.00 | 0.86 | −0.41 |
| GMS 6 | 2.29 | 1.20 | 1.91 | 2.11 | 0.20 | 0.71 | 0.56 |
| GMS 7 | 3.55 | 1.19 | 2.98 | 3.17 | 0.10 | 1.12 | 0.72 |
| GMS 8 | 2.81 | 1.10 | 2.54 | 2.64 | 0.07 | 0.93 | 0.81 |
| GMS 9 | 2.93 | 1.48 | 1.84 | 2.32 | 0.60 | 0.82 | 0.22 |
| GMS 10 | 1.93 | 1.51 | 1.28 | 1.79 | 1.80 | 0.54 | −0.25 |
| GMS 11 | 2.01 | 1.51 | 1.33 | 1.84 | 1.50 | 0.57 | −0.18 |
| GMS 12 | 3.75 | 1.11 | 3.39 | 3.50 | 0.05 | 1.20 | 0.84 |
| GMS 13 | 2.33 | 1.49 | 1.56 | 2.05 | 0.90 | 0.69 | 0.05 |
| GMS 14 | 2.96 | 1.72 | 1.71 | 2.43 | 1.00 | 0.88 | −0.01 |
| GMS 15 | 2.47 | 1.60 | 1.55 | 2.15 | 1.10 | 0.74 | −0.03 |
| GMS 16 | 1.80 | 1.61 | 1.12 | 1.73 | 4.90 | 0.51 | −0.62 |
| GMS 17 | 1.33 | 1.17 | 1.14 | 1.31 | 1.20 | 0.23 | −0.09 |
| GMS 18 | 2.10 | 1.75 | 1.20 | 1.95 | 3.70 | 0.63 | −0.51 |
| GMS 19 | 1.95 | 1.59 | 1.23 | 1.82 | 2.60 | 0.56 | −0.38 |
| GMS 20 | 1.84 | 1.67 | 1.10 | 1.77 | 6.70 | 0.53 | −0.68 |
| GMS 21 | 1.79 | 1.61 | 1.12 | 1.73 | 5.20 | 0.50 | −0.62 |
| GMS 22 | 3.61 | 1.07 | 3.35 | 3.42 | 0.03 | 1.17 | 0.89 |
| GMS 23 | 2.14 | 1.26 | 1.65 | 1.91 | 0.40 | 0.63 | 0.35 |
| GMS 24 | 1.47 | 1.36 | 1.22 | 1.58 | 1.60 | 0.35 | −0.28 |
| GMS 25 | 2.11 | 1.50 | 1.41 | 1.91 | 1.20 | 0.61 | −0.08 |
| GMS 26 | 6.15 | 1.59 | 3.62 | 4.21 | 0.20 | 1.51 | 0.45 |
| GMS 27 | 1.99 | 1.28 | 1.56 | 1.84 | 0.50 | 0.57 | 0.29 |
| GMS 28 | 2.05 | 1.73 | 1.18 | 1.91 | 4.00 | 0.61 | −0.53 |
| GMS 29 | 1.43 | 1.17 | 1.21 | 1.38 | 0.80 | 0.29 | 0.09 |
| GMS 30 | 2.14 | 1.10 | 1.95 | 2.05 | 0.10 | 0.68 | 0.75 |
| GMS 31 | 2.25 | 1.21 | 1.85 | 2.06 | 0.20 | 1.40 | 0.52 |
| GMS 32 | 1.62 | 1.11 | 1.45 | 1.56 | 0.20 | 0.41 | 0.55 |

$X > Y > Z$ semi axes of the strain ellipsoid. $r = X/Y + Y/Z - 1$ (Watterson 1968). $k = (X/Y - 1)/(Y/Z - 1)$ (Flinn 1962). $\gamma_0 = 2/3[(\ln X/Y)^2 + (\ln Y/Z)^2 + (\ln Z/X)^2]^{1/2}$. $\nu = (\ln Y^2/XZ)/(\ln X/Z)$ (Hossack 1968).

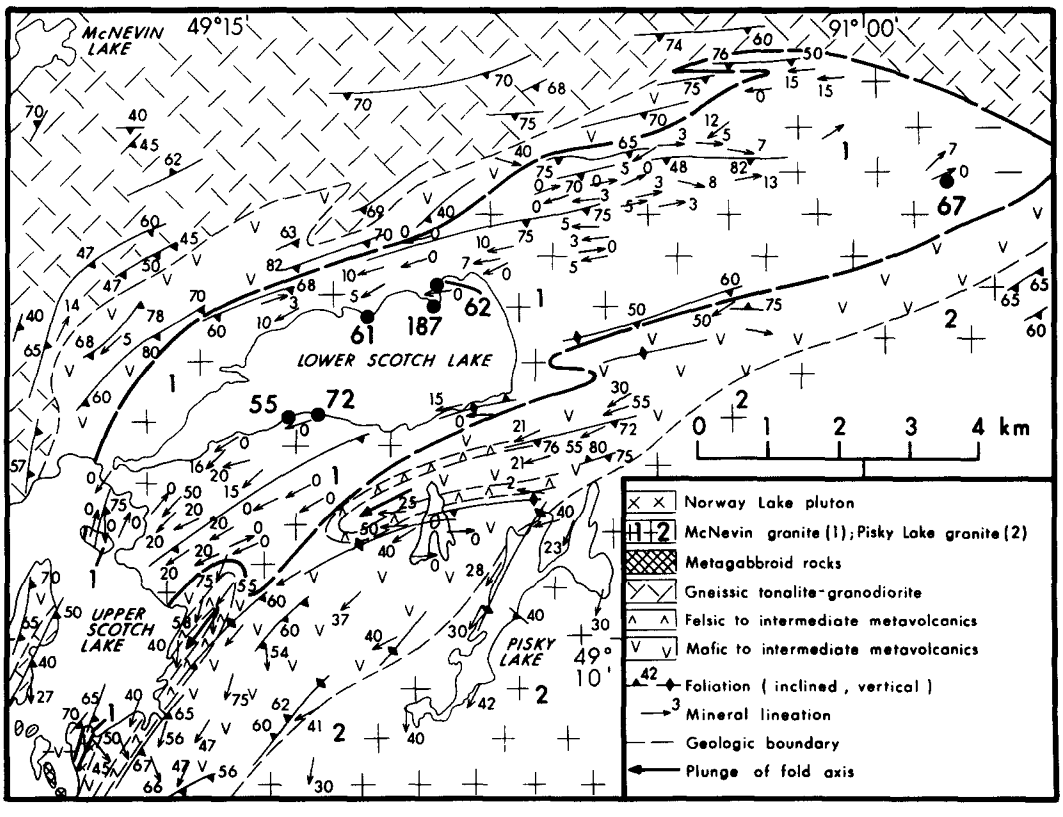


Fig. 5. Lithology and structure of the McNevin Pluton and sample locations of Table 2.

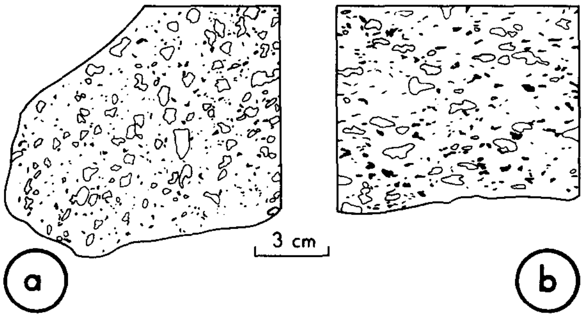


Fig. 6. Strained quartz eyes in McNevin granodiorite, (a) normal to lineation, (b) parallel to lineation.

Elsewhere it generally exhibits a prominent sub-horizontal lineation (Fig. 6) defined by stretched quartz eyes. These recrystallized megacrysts of quartz are excellent strain gauges.

The boundary of each individual quartz eye is assumed to have maintained its integrity at the final stages of intrusion and associated strain. Examination of microstructures in the McNevin granodiorite substantiates this. The strain of the quartz eyes seems to have been accomplished by crystal–plastic deformation. No evidence of widespread diffusive deformation has been observed, though the possibility of minor grain-boundary adjustment (e.g. chemical re-equilibration and grain-shape change) cannot be ruled out. Several granite specimens have been analysed by Robin's (1977) method and various strain parameters calculated (Table 2). The results of this analysis confirm the field estimates of $k$ (Flinn 1962) made by the first author, who mapped the MP and its convex greenstone envelope. The $k$-values are everywhere $>1$ except in the fine-grained granodiorite near the outer intrusive contacts. In many localities, only a quartz-eye lineation can be discerned in the field.

The structure of the concave envelope of the MP, the Scotch Lakes greenstone arm, was mapped by Nowina (1975). Apart from minor intrafolial folds in the primary layering, he mapped several larger folds whose axial traces are subparallel to the greenstone arm (Fig. 5). In contrast to the interior of the MP, mineral stretching lineations within the Scotch Lakes arm have plunges of $>20°$. It would appear that all of these structures predate the MP, and thus the moderate finite strain (Table 2) recorded by the quartz eyes in the McNevin granodiorite.

## JACKFISH–WELLER LAKES PLUTON

In contrast to the McNevin Pluton, the Jackfish–Weller Lakes Pluton (JWLP) has a pronounced constriction in map view (Fig. 8). As suggested in the Introduction, this constriction may be the link between two parasitic lobes that emerged, at a late-plutonic stage, from the large crescentic intrusion.

Sutcliffe (1980) made a geological study of the entire JWLP, but the southwestern portion will not be considered here. We shall give a brief description of the general geology of the pluton before describing its pattern of finite strain.

The JWLP has several compositional variants, but is mainly composed of monzodiorite and monzonite. The

Table 2. Strain analyses, McNevin Pluton

| Sample No. | $X/Z$ | $X/Y$ | $Y/Z$ | $r$ | $k$ | $\gamma_0$ | $\nu$ |
|---|---|---|---|---|---|---|---|
| WMS 79–61 | 2.12 | 1.74 | 1.22 | 1.96 | 1.34 | 0.64 | −0.49 |
| WMS 79–55 | 1.77 | 1.58 | 1.16 | 1.74 | 3.62 | 0.48 | −0.46 |
| WMS 79–67 | 1.47 | 1.37 | 1.07 | 1.44 | 5.30 | 0.33 | −0.64 |
| WMS 74–187 | 1.94 | 1.80 | 1.08 | 1.88 | 10.00 | 0.59 | −0.77 |
| WMS 79–72 | 1.97 | 1.93 | 1.02 | 1.95 | 46.50 | 0.64 | −0.94 |
| WMS 79–62 | 1.98 | 1.75 | 1.13 | 1.88 | 5.77 | 0.59 | −0.64 |

Nomenclature as Table 1.

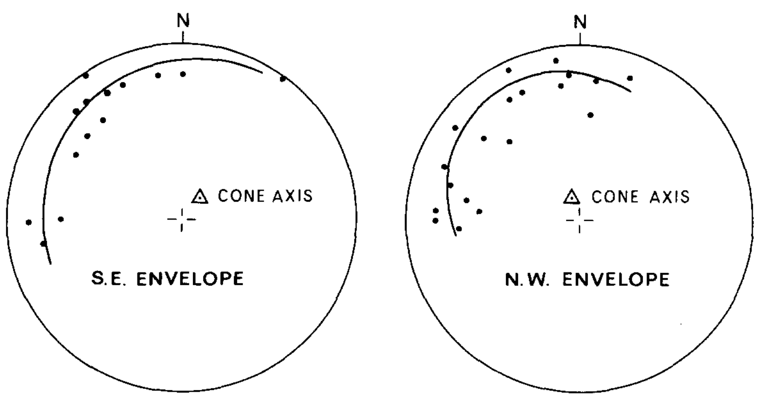


Fig. 7. Small circles, cone axes and hinge lines for boundary zones (metavolcanic envelopes) of McNevin Pluton, as fitted by eye. Apical angles of SE and NW envelopes are 77 and 69°, respectively.

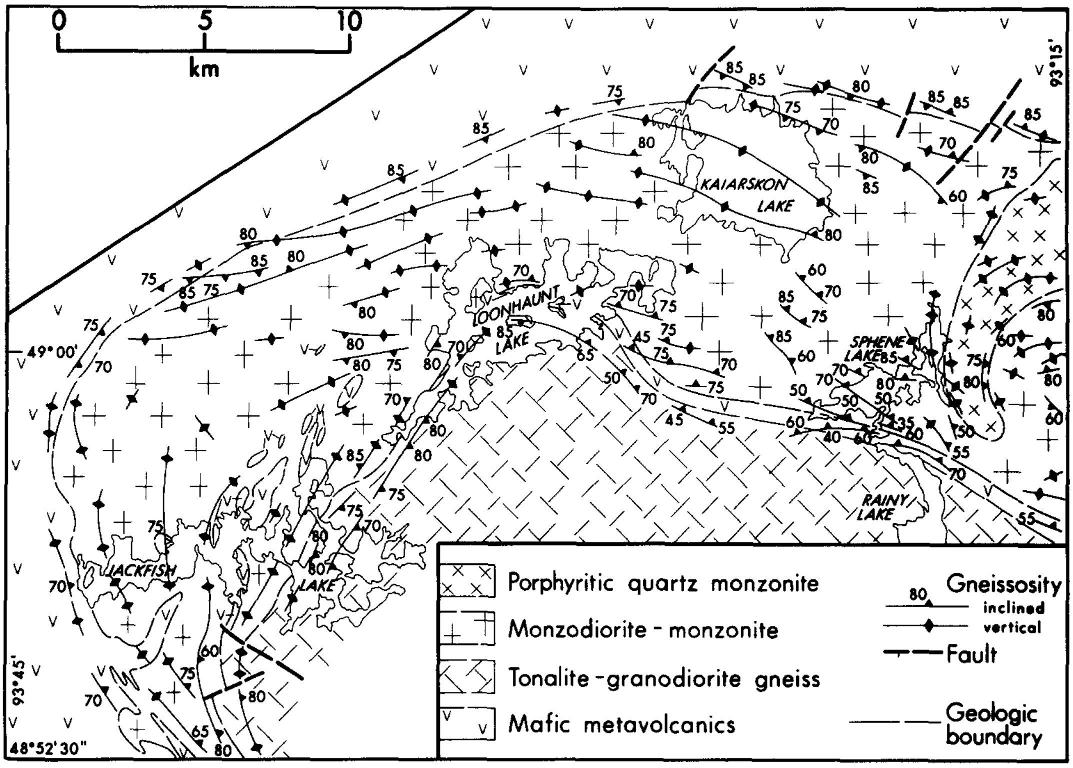


Fig. 8. Lithology and structure of the Jackfish–Weller Lakes Pluton.

JWLP lies between the northern half of the Rainy Lake gneiss diapir (RLGD) and the Kakagi Lake greenstone mass of the Wabigoon Subprovince (Schwerdtner *et al.* 1978a, 1979). On an outcrop scale, the pluton is clearly intrusive into all of its host rocks.

The contact of the Wabigoon metavolcanics is quasi-cylindrical, and its axis plunges at 75°SE toward the RLGD (Sutcliffe 1977, fig. 3a). The cylindrical axis of the subvertical gneissosity at the western boundary plunges southerly at 75°; that is, towards the diapir (Sutcliffe 1977, fig. 3b). In contrast, the cylindrical axis of gneissosity at the northern boundary of the RLGD plunges 55°NE; that is, away from the diapir (Sutcliffe 1977, fig. 3c). Only if the (unknown) dip of this boundary is discordant to gneissosity can the JWLP be regarded as a truly synformal sheet. Foliation attitudes within the pluton (Fig. 8) suggest that such a discordance is likely to be only local, and that the concave boundary of the JWLP may be antiformal. This would imply that, east of the central constriction, the complex is funnel-shaped in cross-section.

Biotite–hornblende aggregates ('mafic clots') of a few millimetres in diameter are evenly distributed in the various plutonic rocks, and constitute excellent gauges of finite strain (Sutcliffe 1977, 1980). These aggregates could be recrystallized phenocrysts or relicts of metavolcanic source rocks in a plutonic melt.

The patterns of $k$-values and strain directions are shown in Figs. 8–10. Strain analyses were performed to test the field estimate of the range of $k$ and to determine the intensity of deformation (Table 3). Two methods of strain analysis were employed (Ramsay 1967, p. 195, and Robin 1977).

Two regions in the JWLP are characterized by $k > 1$ (Fig. 10). Lineations plunge at low angles except near the boundaries of the complex (Fig. 9). Foliations are vertical or steeply inclined in most localities. Most of the smaller dips occur near Sphene Lake (Fig. 8) where the concave contact has a marked overhang and the stretching lineation pitches >50° in the foliation. As might be predicted from the contact attitude, the local strain pattern approaches that of antiformal plutons.

Table 3. Strain analyses, Jackfish–Weller Lake Pluton

| Sample No. | $X/Z$ | $X/Y$ | $Y/Z$ | $r$ | $k$ | $\gamma_0$ | $\nu$ (Hossack 1968) |
|---|---|---|---|---|---|---|---|
| | | | (A) Robin's (1977) Method | | | | |
| S76–25 | 2.29 | 1.61 | 1.42 | 2.03 | 1.45 | 0.68 | −0.15 |
| S76–26 | 2.29 | 1.97 | 1.16 | 2.13 | 6.06 | 0.72 | −0.64 |
| S76–32 | 2.93 | 1.24 | 2.37 | 2.61 | 0.18 | 0.93 | 0.60 |
| | | | (B) Centre-to-centre Method (Ramsay 1967) | | | | |
| S76–25 | 2.66 | 1.90 | 1.40 | 2.30 | 2.20 | 0.82 | −0.31 |
| S76–26 | 3.12 | 2.40 | 1.30 | 2.70 | 4.07 | 0.98 | −0.4 |
| S76–32 | 2.16 | 1.20 | 1.80 | 2.00 | 0.30 | 0.74 | 0.53 |
| S76–29 | 1.00 | 1.00 | 1.00 | 1.00 | — | 0 | — |

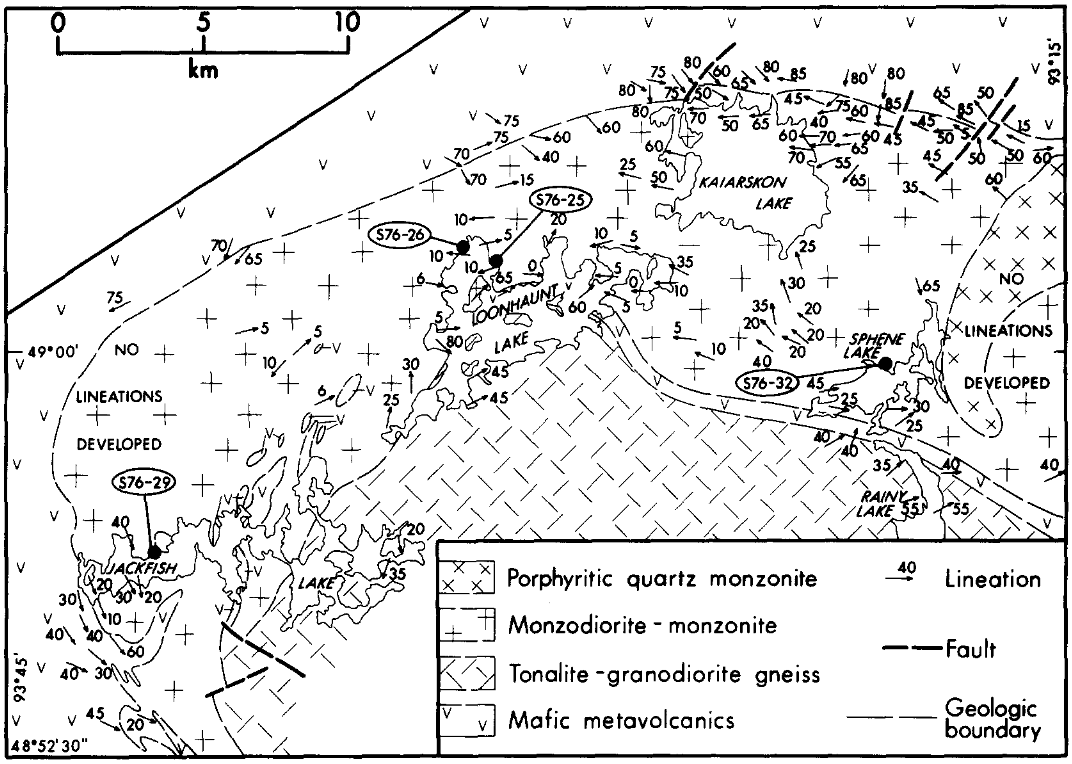


Fig. 9. Lineation pattern and sample locations (Table 3) for the Jackfish–Weller Lakes Pluton.

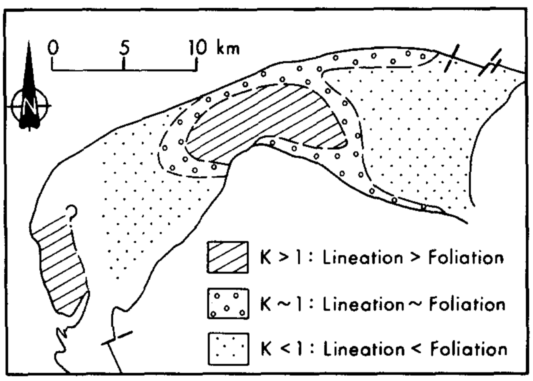


Fig. 10. Pattern of $k$ in the Jackfish–Weller Lakes Pluton.

## VICKERS LAKE PLUTON, A COMPOSITE ANTIFORMAL INTRUSION

Given a level of erosion that is sufficiently high, the advanced lobes of a composite crescentic pluton would be completely separated, on a geological map, by a concordant greenstone envelope. An example of such a structure occurs in the westernmost portion of the Irene–Eltrut Lakes diapir (Schwerdtner & Lumbers 1980), Wabigoon Subprovince. No detailed study of the strain pattern of this situation was undertaken by the authors.

The Vickers Lake Pluton (VLP) is mainly composed of granodiorite (Sage *et al.* 1974). It has a central arm of greenstone which diverges at the concave side of the crescentic pluton to form a prominent septum between gneiss and granitoids (Fig. 11). This setting suggests that the VLP is an antiformal pluton with two advanced lobes.

The southern lobe is much smaller than its northern twin, which is characterized by steep prolate ellipsoids of finite strain. The prolateness factor ($k$) was crudely estimated in the field and later confirmed by magnetic fabric measurements.

The high $k$-values are not only reflected in the mineral fabric (mafic clots and feldspar megacrysts) but also in the shape of ellipsoidal mafic xenoliths (5–20 cm in diameter), which are invariably parallel to the lineation and foliation. In some locations, the attitude of the weak mineral fabric is most readily obtained by measuring the orientation of the aligned xenoliths. Commonly, no mineral fabric can be discerned in the field. Thus, the mineral fabric appears to gauge a smaller increment of late-plutonic strain than the xenolith fabric.

## INTERPRETATION OF NATURAL STRAIN PATTERNS

Figure 12 shows generalized strain patterns of simple crescentic structures like the Greenwater and McNevin Plutons. Three ways of generating the forms and strain patterns of such plutons will be considered here: (1) diapiric bending of horizontal sills originally intruded between a gneiss complex and its greenstone cover; (2) expansion of undeformed crescentic plutons in a late pulse of spasmodic gneiss doming and (3) ascent of granitoid material at (or near) the contact of stable gneiss domes.

### *Bending of granitoid sills*

The horizontal-sill hypothesis can be tested by using

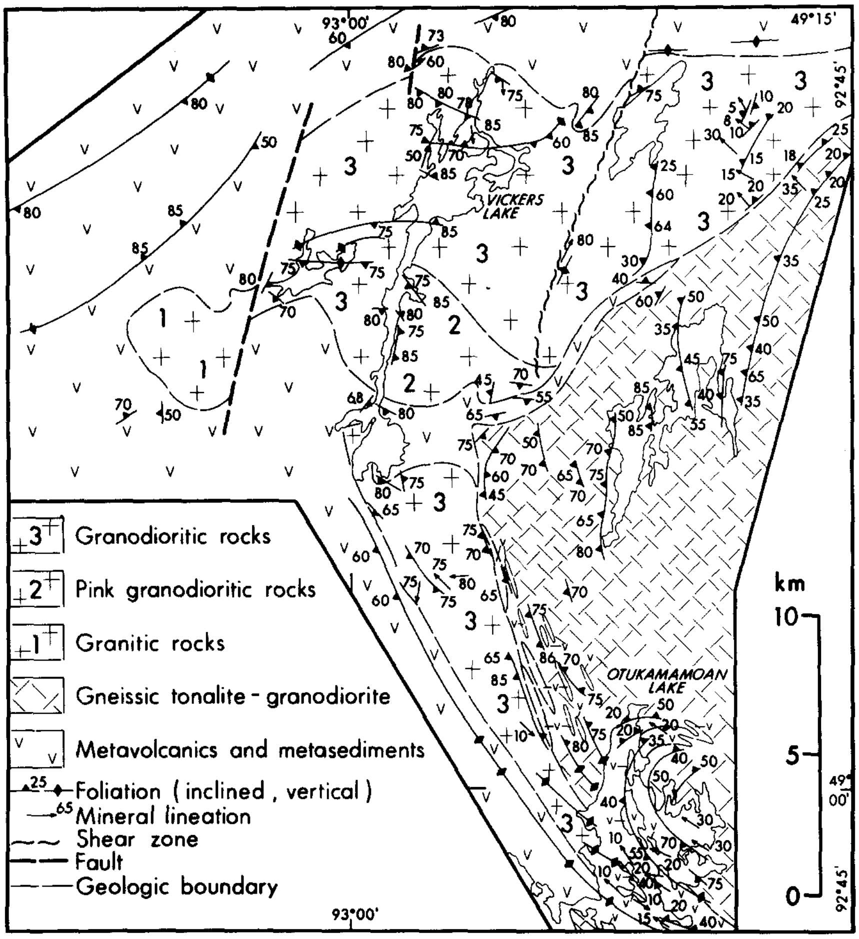


Fig. 11. Lithology and structure of the Vickers Lake Pluton.

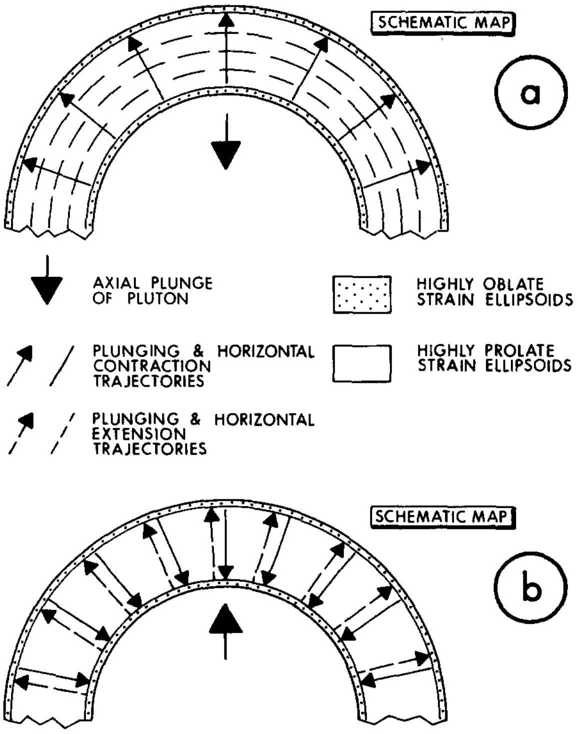


Fig. 12. Generalized strain patterns of simple natural plutons, (a) synformal pattern, (b) antiformal pattern.

published model patterns of cumulative diapiric strain (Fletcher 1967, 1972, Dixon 1975), and assuming that the original granitoid sill had the same physical properties as the basement gneiss. Fletcher (1967, 1972) was the only worker to study the strain pattern of circular diapirs, but he did not consider the advanced stage of 'mushrooming' in mature structures. Dixon (1975) modelled the biaxial-strain field of mature and immature diapiric ridges, and discussed the non-trivial adaptation of the biaxial strains to the triaxial deformation in diapiric domes. His suggested adaptation is purely qualitative, as is Fletcher's (1972) 'intrastratal' model to be referred to below.

Only the strains in the outer shell of model domes and adjacent host material need to be considered here. Because of the presence of an arcuate surface of no longitudinal strain in many diapiric models (Schwerdtner *et al.* 1978b), the strain of the outer shell of diapirs tends to be akin to that of the adjacent host material.

Recall that antiformal plutons occur near the outward-dipping contacts of gneiss domes. At this structural site in the diapiric models, the cumulative deformation of the buoyant substance as well as the adjacent overburden material is represented by *oblate* strain ellipsoids (Fletcher 1972, p. 208, Dixon 1975, p. 122). This type of strain disagrees with the prevailing constrictive deformation in natural antiformal plutons (Fig. 12). Similarly,

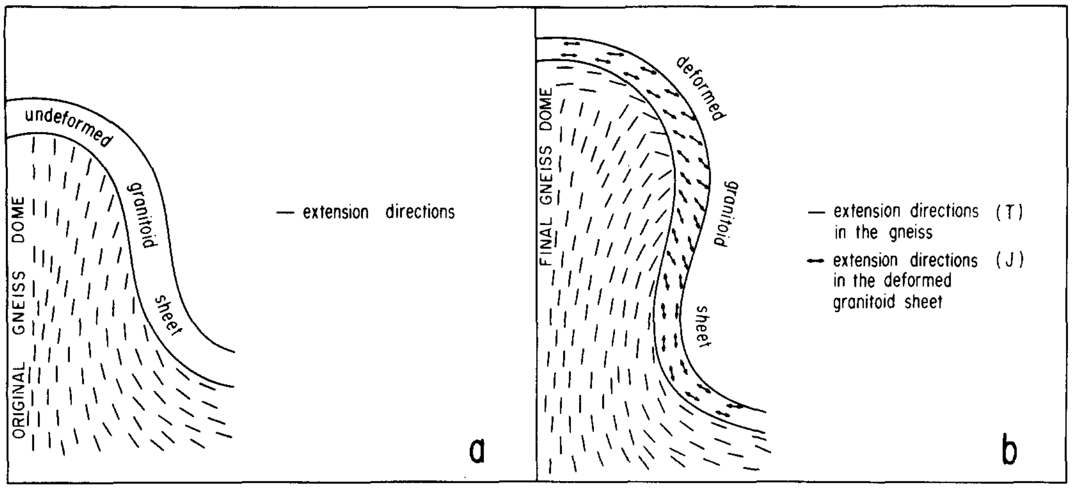


Fig. 13. Reactivation of a gneiss diapir with unstrained plutonic hood (after two-dimensional models by Dixon 1975, and Carey 1979); (a) undeformed plutonic hood, (b) stretched plutonic hood in vertical section.

the strain ellipsoids near the overhang of mature diapirs, with which synformal plutons are generally associated, should be strongly oblate. This can be seen by combining the simultaneous components of subvertical extension apparent in Dixon's (1975) biaxial models with those of circumferential-horizontal extension discussed by Fletcher (1972, p. 209) and Dixon (1975, p. 122). Again, the oblate strain ellipsoids of the qualitative diapiric models disagree with the prolate ellipsoids that dominate the natural strain patterns. Moreover, a bending strain cannot lead to the symmetric zonation of the generalized natural pattern of simple crescentic plutons (Fig. 12). This seems to rule out the possibility that the crescentic plutons were bent together with the greenstone mantle of typical gneiss domes.

*Expansion of undeformed crescentic plutons*

Let us now consider the hypothesis that the finite strain in the natural crescentic plutons has been generated by the expansion of consolidated but undeformed granitoid hoods (Fig. 13) or partial-hoods around growing gneiss diapirs. This case of spasmodic diapirism may be treated by considering the large incremental deformation (Carey 1979) of the outer shell of one of Dixon's (1975) two-dimensional models. Note the quasi-concordant pattern of extension directions in deformed cylindrical plutons (Fig. 13). To adapt this pattern to axially-symmetric plutons, we must allow for circumferential as well as subvertical extension in the outer shells of expanding circular domes. The inferred three-dimensional deformation pattern is characterized by oblate strain ellipsoids, which are again at variance with the constrictive strains and the symmetrical zonation in the generalized strain patterns of simple natural plutons (Fig. 12).

*Ascent of plutonic material along the contact of stable gneiss domes*

Depending on the shape and location of the region of melting, we envisage three situations: (a) generation of magma at, and subsequent rise of magma along, the contact of gneiss domes; (b) injection of ascending magma into, and further rise along, the gneiss–greenstone contact and (c) uniform melting at an appropriate level in the crust and rise of arcute diapiric ridges along the contact of stable gneiss domes (Fig. 14). Owing to the steep contacts of most arcuate plutons, situation (c) must be included in the list.

If one assumes that the strain recorded by the mineral aggregates represents the last major increment of plutonic flow, it becomes impossible to distinguish between situations (a) and (b). A distinction cannot even be made on the basis of strained mafic xenoliths, because they could have been incorporated into the magma at any stage of ascent. Figure 15 illustrates qualitatively how one can account for the principal difference between the antiformal and synformal strain patterns (Fig. 12) of simple crescentic plutons. No attempt is made to explain the oblate strain ellipsoids near the margins of the crescentic plutons (Fig. 12). This cannot be accomplished on the basis of purely kinematic models that specify neither the boundary conditions between, nor the rheologic states of, plutonic material and wall rocks.

Situation (c) can be readily eliminated from consideration by comparing Fig. 12 with Figs. 16(a) & (b). As pointed out in a previous paper (Schwerdtner & Troëng 1978), the asymmetric patterns of total as well as incremental strain in arcuate diapiric ridges of silicone putty are fairly complicated, and differ markedly from the natural strain patterns of simple crescentic plutons (Fig. 12). While the rheologic contrast between putty and nearly-consolidated felsic magma may account for part of that difference, we attach more significance to the bilateral supply of diapiric material (Fig. 14). This bilateral supply is also responsible for the outward-dipping contacts of the diapiric ridges (Fig. 14), which are at variance with the subparallel boundaries of natural crescentic plutons.

Let us now turn to composite plutons like the syn-

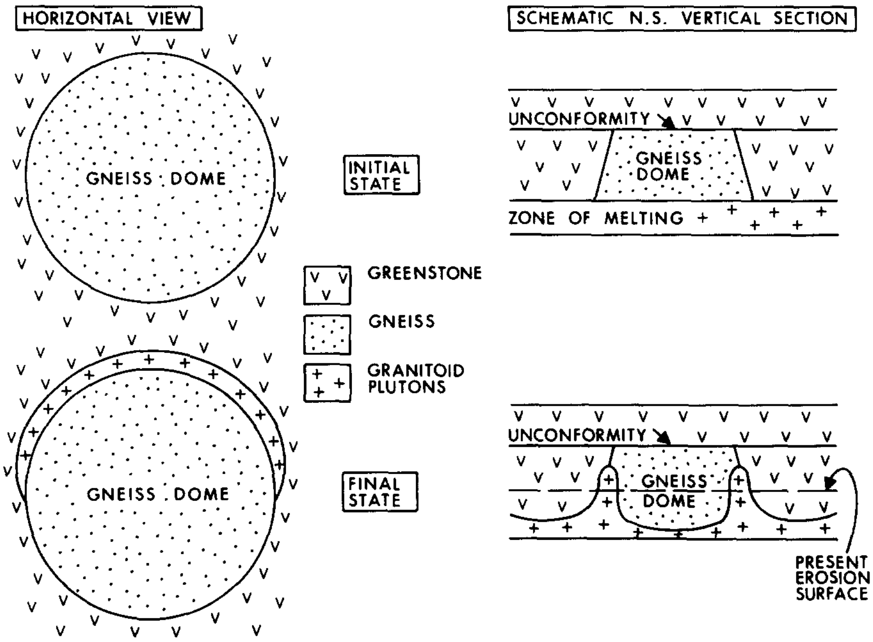


Fig. 14. Hypothetical evolution of arcuate diapiric plutons with outward-dipping contacts (schematic sketches).

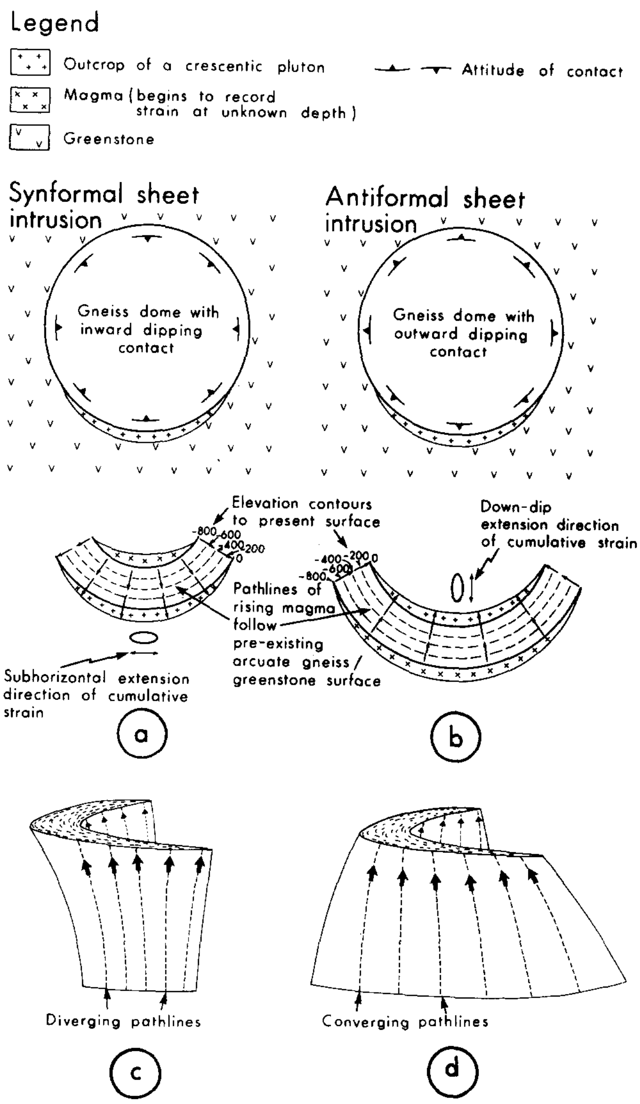


Fig. 15. Magma generation at, and magma ascent along, the gneiss–greenstone interface of domes. Flow regimes and inferred strain patterns of (a) simple synformal plutons and (b) simple antiformal plutons; (c) and (d) are the respective flow regimes in three dimensions.

formal JWLP (Fig. 8) and the antiformal VLP (Fig. 11). Their parasitic structures are either teardrop-shaped twin domes that have emerged from an arcuate diapiric ridge (Gould & DeMille 1964, p. 729) or tongue-shaped lobes of quasi-concordant sheets.

A critical region in the strain field of the JWLP is centred about the western half of Jackfish Lake. This oval domain is near the southwestern end of the complex and should have subvertical lineations if it is a conventional diapir (cf. Ramberg 1963, fig. 9, Fletcher 1967).

Ramberg (1967) and Schwerdtner & Troëng (1978) made appropriate diapiric models whose horizontal outline resembles that of the JWLP. Schwerdtner & Troëng (1978, model WMS 20) determined the triaxial strain pattern of the constriction zone, whereas Ramberg (1967 fig. 71) studied the component of horizontal longitudinal strain parallel to the diapiric contact. He showed that the region of constriction is characterized by horizontal stretching and the end regions of an arcuate diapiric ridge have the strain pattern of circular diapirs (i.e. circumferential shortening and down-dip radial extension).

Figures 8–10 show that, while $k > 1$, the stretching lineation around western Jackfish Lake is far from being subvertical. In spite of very steep contacts, the local strain pattern is that of a synformal pluton (Fig. 12) rather than a conventional diapir. Although the strain pattern of the neck region of the JWLP is compatible with the synformal model of Fig. 15, the horizontal lineation was probably accentuated by the bilateral flow of monzonite from the zone of constriction into the advancing lobes.

## SUMMARY AND CONCLUSIONS

Three principal mechanisms of generating the forms and strain patterns of Archean crescentic plutons were

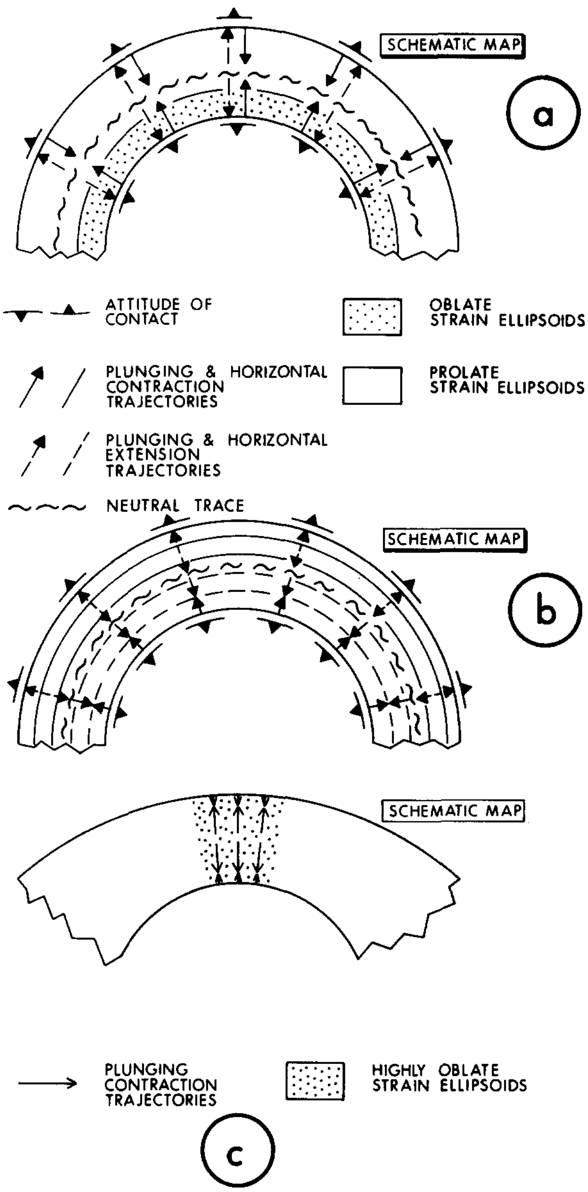


Fig. 16. Strain patterns of experimental arcuate diapirs with (a) low amplitude and (b) higher amplitude; (c) strain pattern in a depressed ridge between two second-order domes (after Schwerdtner & Troëng 1978).

considered: (1) diapiric bending of horizontal sills between basement gneiss and greenstone cover; (2) tectonic expansion of undeformed crescentic plutons and (3) plutonic ascent of granitoid material at the contact of stable gneiss domes, either as plunging conical sheets (a, b) or as vertical diapiric ridges (c).

Only mechanism 3a,b produces the symmetric zonation of the generalized strain patterns of simple crescentic plutons (Fig. 12). None of the natural strain fields of the four crescentic plutons studied proved to be compatible with mechanisms 1, 2 and 3c. In spite of the simplistic models employed, mechanism 3a,b accounts for most elements of the natural strain patterns. In view of the kinematic nature of these models, which fail to predict the strain near the sheet boundaries, it was impossible to interpret the oblate strain ellipsoids in the contact regions of the natural crescentic plutons.

The results of the strain study agree with the structural history of the various Archean rocks as reconstructed from general geological evidence (for details, cf. Introduction). We thus conclude that the crescentic plutons rose along the arcuate interface between stable gneiss domes and their greenstone envelopes.

Low to moderate strain intensities are found within the plutons, and contrast sharply with the prevailing high strain levels in the gneiss domes (Schwerdtner *et al.* 1978b and unpublished data). Apparently, the strains recorded in the plutons were imposed on nearly consolidated granitoid material, at the final stages of buoyant ascent.

*Acknowledgements*—This project was supported by EMR and NSERC grants to the senior author (W.M.S.). The work of G.M.S. and R.H.S. was mainly supported by the Ontario Geological Survey. Mike Donnan and Jean van Berkel plotted some of the field data and sketched the geological maps. Thanks are also due to C. K. Mawer, who examined the textures of deformed plutonic rocks, and to C. T. Talbot, who offered constructive advice in his official review.

## REFERENCES

Blackburn, C. E. 1981. Kenora-Fort Frances sheet (Geological Compilation Series), Ont. Geol. Surv. Map 2443, scale 1:253440.

Carey, P. D. 1979. Incremental strain in diapiric ridge structures. Unpub. B.Sc. thesis, Fac. Appl. Sci., Queen's University, Kingston, Ontario.

Dixon, J. M. 1975. Finite strain and progressive deformation in models of diapiric structures. *Tectonophysics* **28**, 89–124.

Fletcher, R. C. 1967. A finite amplitude model for the emplacement of gneiss domes. Ph.D. thesis, Brown University, Providence, R.I.

Fletcher, R. C. 1972. A finite amplitude model for the emplacement of mantled gneiss domes. *Am. J. Sci.* **272**, 197–216.

Flinn, D. 1962. On folding during three dimensional progressive deformation. *Q. Jl geol. Soc. Lond.* **118**, 385–433.

Gould, D. B. & DeMille, G. 1964. Piercement structures in the Arctic Islands. *Bull. Can. Petrol. Geol.* **12**, 719–753.

Hossack, J. B. 1968. Pebble deformation and thrusting in the Bydin area (southern Norway). *Tectonophysics* **5**, 315–339.

Nowina, S. F. 1975. Structure of the Scotch Lakes area. In: *Geotraverse Workshop Proceedings*, Department of Geology, University of Toronto, pp. 149–150.

Ramberg, H. 1963. Strain distribution and geometry of folds. *Bull. geol. Instn. Univ. Uppsala* **42**, 1–20.

Ramberg, H. 1967. *Gravity, Deformation and the Earth's Crust.* Academic Press, London.

Ramsay, J. G. 1967. *Folding and Fracturing of Rocks.* McGraw-Hill Book Company, New York, NY.

Robin, P.-Y. F. Determination of geologic strain using randomly oriented strain markers of any shape. *Tectonophysics* **42**, T7–T16.

Sage, R. P., Breaks, F. W., Stott, G. M., McWilliams, G. M., 1974. Operation Ignace-Armstrong, Preliminary geological maps P962–P965 (Paskokogan-Caribou Lakes Sheet, Obanga Lake-Lac Des Isle Sheet, Ignace-Graham Sheet and Mine Centre Sheet). Ontario Division of Mines. Scale 1 inch = 1 mile.

Schwerdtner, W. M. 1978. Strain patterns within conformable granitoid bodies of the Superior and Grenville Provinces, northwestern and southwestern Ontario. Geological and Mineralogical Association of Canada, Abstracts with Programs 3, 488.

Schwerdtner, W. M. 1982. Salt stocks as natural analogues of Archean gneiss diapirs. *Geol. Rdsch.* **71**, 370–379.

Schwerdtner, W. M., Morgan, J., Osadetz, K., Stone, D., Stott, G. M. & Sutcliffe, R. H. 1978a. Structure of Archean rocks in western Ontario. In: *Proceedings of the 1978 Archean Geochemistry Conference*, University of Toronto Press.

Schwerdtner, W. M., Sutcliffe, R. H. and Troëng, B. 1978b. Patterns of total strain within the crestal region of immature diapirs. *Can. J. Earth Sci.* **15**, 1437–1447.

Schwerdtner, W. M. & Troëng, B. 1978. Strain distribution within arcuate diapiric ridges of silicone putty. *Tectonophysics* **50**, 13–28.

Schwerdtner, W. M., Stone, D., Osadetz, K., Morgan, J. & Stott, G. M. 1979. Granitoid complexes and the Archean tectonic record in the southern part of northwestern Ontario, *Can. J. Earth Sci.* **16**, 1965–1977.

Schwerdtner, W. M. & Lumbers, S. B. 1980. Major diapiric structures in the Superior and Grenville Provinces of Ontario. *Spec. pap. Geol. Ass. Can.* **20**, 149–180.

Stott, G. M. & Schwerdtner, W. M. 1980. Structural analysis of the central part of the Shebandowan metasedimentary-metavolcanic belt. Ont. Geol. Survey, Open File report 5349.

Sutcliffe, R. H. 1977. Geology and emplacement of the Jackfish Lake Pluton, a major intrusion in the Rainy Lake dome. In: *Proceedings of the 1977 Geotraverse Conference*, Precambrian Research Group, University of Toronto, Toronto, Ont., pp. 146–154.

Sutcliffe, R. H. 1980. Evolution of the Rainy Lake granitoid complex, northwestern Ontario. Unpublished M.Sc. thesis, Dept. of Geology, University of Toronto.

Watterson, J. 1968. Homogeneous deformation of the gneisses of Vesterland, southwest Greenland. Bull. Gronlands Geol. Unders. **78**.

Woolverton, R. S. 1960. Geology of the Lumby Lake Area, District of Thunder Bay, Ont. Dept. Mines, v. 69, pt. 5.